# Influence of Freestream Values on $k$-$\omega$ Turbulence Model Predictions

F. R. Menter*
*Eloret Institute, Palo Alto, California 94303*

## Introduction

TWO equation eddy-viscosity turbulence models are among the most widely used models today. The most popular is the $k$-$\epsilon$ model in one of its many different forms. However, a significant number of alternative models have been developed, both for physical and for numerical reasons. Those models are designed to overcome some of the well-known shortcomings of the $k$-$\epsilon$ model.

One of the more successful of the alternative models is the $k$-$\omega$ model developed by Wilcox.[1,2] It has the advantage that it does not require damping functions in the viscous sublayer and that the equations are less stiff near the wall. Furthermore, it has been designed to predict the proper wake strength in equilibrium adverse pressure gradient boundary-layer flows.

Very encouraging results for a variety of wall-bounded flows have been reported by different authors.[1-3] However, when applied to free shear layers, a strong dependency of the results on the freestream value of $\omega$ has been found.[2] To investigate this disturbing feature of the equations more closely, the self-similar equations for incompressible equilibrium boundary layers, as well as for the far wake, have been solved numerically. Different freestream values $\omega_f$ have been specified to determine its influence on the solution. From the self-similar equations one can also get estimates for acceptable values of $\omega_f$. To show that the solution dependency of $\omega_f$ is not simply a property of the self-similar equations, Navier-Stokes computations have been performed for a flat plate boundary layer that confirm the results.

## Defect Layer and Far Wake Analysis

Wilcox has performed a defect layer analysis for the $k$-$\omega$ model to investigate the model performance for equilibrium boundary-layer flows. The analysis is based on a singular perturbation solution with respect to the (small) ratio of the friction velocity to the boundary-layer edge velocity $u_\tau/U_e$. It is further assumed that the Reynolds number based on displacement thickness is high, $Re_{\delta^*}\rightarrow\infty$. The equations prescribing the self-similar far wake flow are identical to the equations derived by Wilcox, if $u_\tau$ is replaced by $u_1 = U_e\sqrt{\delta^*/x}$. The details of the analysis can be found in Ref. 1, and therefore only a brief summary of the equations is given here. The defect layer and far wake equations are as follows:

$$\frac{\partial}{\partial\eta}\left[N_0\frac{\partial U_1}{\partial\eta}\right] + (\alpha_T - 2\beta_T - 2\omega_T)\eta\frac{\partial U_1}{\partial\eta} + (\beta_T - 2\omega_T)U_1 = 0$$

$$\sigma^*\frac{\partial}{\partial\eta}\left[N_0\frac{\partial K_0}{\partial\eta}\right] + (\alpha_T - 2\beta_T - 2\omega_T)\eta\frac{\partial K_0}{\partial\eta} - 4\omega_T K_0 + \sqrt{\beta^*}\left[N_0\left(\frac{\partial U_1}{\partial\eta}\right)^2 - K_0W_0\right] = 0$$

$$\sigma\frac{\partial}{\partial\eta}\left[N_0\frac{\partial W_0}{\partial\eta}\right] + (\alpha_T - 2\beta_T - 2\omega_T)\eta\frac{\partial W_0}{\partial\eta} + (\alpha_T - \beta_T - 4\omega_T)W_0 + \sqrt{\beta^*}\left[\gamma\left(\frac{\partial U_1}{\partial\eta}\right)^2 - \frac{\beta}{\beta^*}W_0^2\right] = 0 \tag{1}$$

Received Sept. 3, 1991; revision received Oct. 7, 1991; accepted for publication Oct. 10, 1991. This paper is declared a work of the U.S. Government and is not subject to copyright protection in the United States.

*Research Engineer; mailing address: Experimental Fluid Dynamics Branch, NASA Ames Research Center, MS 229-1, Moffett Field, California 94035. Member AIAA.

where $U_1$, $K_0$, and $W_0$ are the nondimensional defect velocity, turbulent kinetic energy, and turbulent dissipation rate $\omega$, respectively. $N_0$ is the dimensionless eddy viscosity:

$$N_0 = \frac{\nu_t}{U_e\delta^*} = \frac{K_0}{W_0} \tag{2}$$

whereas $\alpha_T$, $\beta_T$, and $\omega_T$ are defined as follows:

$$\alpha_T = \frac{2}{C_f}\frac{d\delta^*}{dx}, \quad \beta_T = \frac{\delta^*}{\tau_w}\frac{dp}{dx}, \quad \omega_T = \frac{\delta^*}{C_f u_\tau}\frac{du_\tau}{dx} \tag{3}$$

where $\delta^*$ is the displacement thickness, $\tau_w$ is the wall shear stress, and $C_f/2 = (u_\tau/U_e)^2$. The values of these quantities for a zero pressure gradient boundary layer are $\alpha_T = 1$, $\beta_T = 0$, and $\omega_T = 0$. For the wake flow, they are: $\alpha_T = 0$, $\beta_T = 0$, $\omega_T = -0.25$.

The constants in the $k$-$\omega$ model are

$$\beta = 3/40,\ \beta^* = 0.09,\ \kappa = 0.41,\ \gamma = 5/9,\ \sigma = 0.5,\ \sigma^* = 0.5 \tag{4}$$

For boundary-layer applications, the equations must be matched to the law of the wall,[1] whereas symmetry conditions are imposed on the wake centerline. At the outer boundary $\eta\rightarrow\infty$, all three quantities are assigned small values:

$$U_1 = 0, \quad K_0 = K_f, \quad W_0 = W_f \tag{5}$$

The equations are solved with a first-order upwind scheme for the convection terms $\eta(\partial/\partial\eta)$ and central differencing for the other derivatives. Following Wilcox,[1] time derivatives are added to integrate the equations. Highly accurate numerical results were obtained by using up to 500 gridpoints in $\eta$. Grid independency was reached with about 100 gridpoints inside the layer.

## Results

The equations have been solved with different freestream values $W_f$ specified. Note that the $W_0$ equation has two different algebraic solutions in the freestream that are compatible with the equilibrium assumption. One is $W_f = 0$ and the second is

$$W_f =: W_a = (\alpha_T - \beta_T - 4\omega_T)\frac{\sqrt{\beta^*}}{\beta} \tag{6}$$

Although intermediate values are not strictly compatible with the equilibrium assumptions, they will be included to show the changes of the solution as $W_f$ approaches zero (setting $W_f$ exactly to zero is not possible for numerical reasons).

Computations show that specification of values for $W_f$ larger than $W_a$ does not influence the results, as $W_0$ falls to $W_a$ at the boundary-layer edge before approaching $W_f > W_a$ outside the boundary layer. However, specifying smaller values has a pronounced influence. Computations have been performed with

$$W_f = W_a\cdot 10^{-n}, \qquad n = 0, 1, 2, \ldots \tag{7}$$

The value of $K_f$ was changed in a way to keep the freestream value of the eddy viscosity at a low value of $N_f = 10^{-4}$ (changes in $N_f$ do not affect the solution, as long as it is small compared with the values of $N_0$ inside the boundary layer). Figure 1 shows the results for the equilibrium boundary-layer computations. The influence of $W_f$ on the solution can be seen most dramatically with regard to the eddy viscosity $N_0$. $N_0$ increases as $W_f$ decreases and does not go to zero at the boundary-layer edge $\delta_{0.995}$. The influence on the mean flow profile $U_1(\eta)$ is moderate, and that is the reason why the freestream dependency is of little consequence for boundary-layer flows. However, near the boundary-layer edge the solution changes from a profile with a sharply defined boundary-

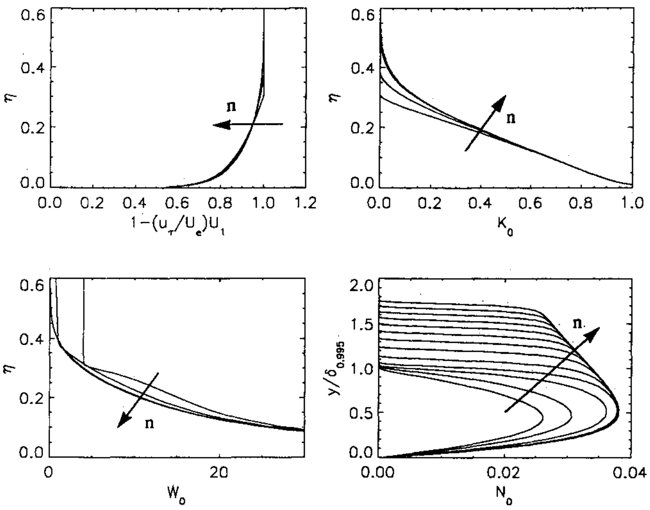


**Fig. 1 Solutions of the defect layer equations with different freestream values for $W_0$, $W_f = W_a 10^{-n}$, $n = 0, 1, 2, 3, \ldots$**

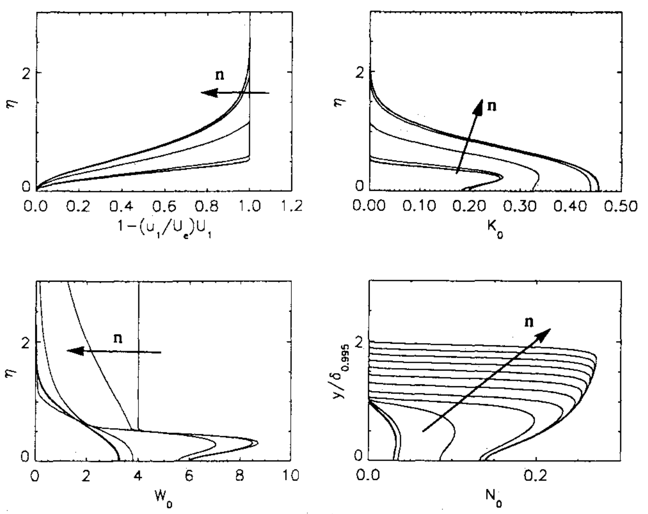


**Fig. 2 Solutions of the far wake equations with different freestream values for $W_0$, $W_f = W_a 10^{-n}$, $n = 0, 1, 2, 3, \ldots$**

layer edge, to one that approaches the freestream values asymtotically as $W_f$ decreases.

Figure 2 shows the solution for wake flows. The changes in $N_0$ are similar to the ones for the boundary-layer computations, only now the whole shear layer is affected because of the missing wall influence. The velocity profile is also strongly affected and shows a much larger spreading rate as $W_f$ decreases. Again the sharp edge of the shear layer is lost, and all variables approach their freestream values asymtotically.

Analysis of the defect layer equations shows[4,5] that two equation models generally produce solutions with a sharp boundary-layer edge (discontinuous in the first derivatives). This is also true for the design solution of the $k$-$\omega$ model if $W_f = W_a$. However, for the limiting case $K_f = 0$ and $W_f = 0$, no such solution exists and the solution for large $\eta$ becomes

$$U_1 = C_1 e^{-\lambda\eta^2}$$
$$K_0 = C_2 e^{-\lambda^*\eta^2}$$
$$W_0 = C_3 e^{-\lambda^*\eta^2} \tag{8}$$

The exponents are

$$\lambda = (\alpha_T - 2\beta_T - 2\omega_T)/(2N_0)$$
$$\lambda^* = (\alpha_T - 2\beta_T - 2\omega_T)/[2N_0\sigma^{(*)}] \tag{9}$$

Since $\sigma$ is equal to $\sigma^*$, $K_0$ and $W_0$ decay in the same manner, allowing for a constant eddy viscosity $N_0 = C_2/C_3$ (see Fig. 2). Note that the previous solution exists only if $\sigma = \sigma^*$. If $\sigma$ is not equal to $\sigma^*$, the solution has a sharp boundary-layer edge, but a strong dependency of $\omega_f$ remains.

Computations with the $k$-$\epsilon$ model for the previous cases show almost no dependency on the freestream values. As pointed out in Refs. 1 and 6, the main difference between both models is a term of the form

$$2(\nu + \sigma\nu_t)\frac{1}{k}\frac{\partial k}{\partial x_i}\frac{\partial \omega}{\partial x_i} \tag{10}$$

that is not included in the $\omega$ equation (note that an additional diffusion term appears if the diffusion constants are not equal). In the self-similar limit, the expression in Eq. (10) becomes

$$2\sigma N_0 \frac{1}{K_0}\frac{\mathrm{d}K_0}{\mathrm{d}\eta}\frac{\mathrm{d}W_0}{\mathrm{d}\eta} \tag{11}$$

and has to be added to the left-hand side of the $W_0$ equation.

Figure 3 shows computations for the wake flow with this term included in the $k$-$\omega$ model. The main difference is that the influence of $W_f$ does not penetrate into the boundary layer. The freestream dependency is thereby avoided. The computations shown in Fig. 3 have been performed with the constants of the Jones-Launder $k$-$\epsilon$ model transformed to the $k$-$\omega$ model (the freestream dependency is also removed if the original constants are used).

The inclusion of the term in Eq. (10), however, is not desirable because it makes the $k$-$\omega$ model formally identical to the $k$-$\epsilon$ model and thereby destroys the advantages of the model in the near wall region and for adverse pressure gradient boundary layers.

The argument can be made that the previous findings are specific features of the self-similar equations and do not appear if the full equations are solved. To investigate this point, flat plate boundary-layer computations based on the incompressible Reynolds-averaged Navier-Stokes equations have been performed. The freestream value $\omega_f$ at the inflow boundary was reduced to small values (note that the freestream value of $k$ was also reduced to keep the eddy viscosity in the freestream small). The results are almost identical to the ones shown in Fig. 1, thus providing further evidence that the similarity solutions capture the essence of the problem.

The present results show that it is very important to specify $\omega_f$ appropriately at the inflow boundary. In cases where the freestream values inside the computational domain cannot be

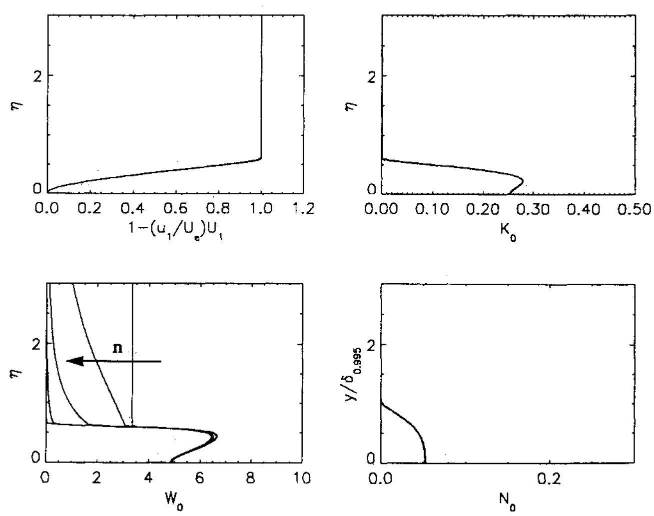


**Fig. 3 Solutions of the far wake equations with different freestream values for $W_0$, $W_f = W_a 10^{-n}$, $n = 0, 1, 2, 3, \ldots$, $2\sigma N_0(1/K_0)$ $(\mathrm{d}K_0/\mathrm{d}\eta)$ $(\mathrm{d}W_0/\mathrm{d}\eta)$ is included in the $W_0$ equation.**

sufficiently controlled by the inflow conditions alone, it may be even necessary to impose a lower limit on $\omega$. Estimates for those values can be obtained from the definition of $W_0$ (Ref. 1) and from Eq. (6):

$$\omega = \frac{u_\tau^2}{\sqrt{\beta^*} U_e \delta^*} W_0(\eta)$$
$$\omega_a = \frac{1}{\beta} \frac{u_\tau^2}{U_e \delta^*} (\alpha_T - \beta_T - 4\omega_T) \tag{12}$$

For high Reynolds number boundary-layer flows, this gives the following estimate:

$$\omega_a = \frac{1}{\beta} \frac{1}{\delta^*} \frac{\mathrm{d}}{\mathrm{d}x} (U_e \delta^*) = \mathcal{O}\left(10 \frac{U_\infty}{L}\right) \tag{13}$$

where $U_\infty$ is the freestream velocity and $L$ is a characteristic length in the streamwise direction. In high Reynolds number boundary-layer applications, these rather large values can be specified because $\omega$ inside the layer in still several orders of magnitude larger and $\omega_f$ is therefore relatively small. It is the author's experience that the freestream dependency is no major problem in boundary-layer computations and can be avoided by specifying appropriate inflow conditions and/or lower limits on $\omega$.

The problem is more severe in free shear layer applications in which case the freestream value $W_a$ is of the same order as $W_0$ (see Fig. 2) inside the layer, and therefore it is not appropriate to impose a lower limit. The inclusion of additional terms in the $\omega$ equation or changes in the expression for the eddy viscosity might be necessary to ensure solutions that are both insensitive to $\omega_f$ and consistent with experiments.

## References

[1]Wilcox, D. C., "Reassessment of the Scale-Determining Equation for Advanced Turbulence Models," *AIAA Journal*, Vol. 26, No. 11, 1988, pp. 1299–1310.

[2]Wilcox, D. C., "A Half Century Historical Review of the $k$-$\omega$ Model," AIAA Paper 91-0615, Jan. 1991.

[3]Menter, F. R., "Performance of Popular Turbulence Models for Attached and Separated Adverse Pressure Gradient Flows," AIAA Paper 91-1784, June 1991.

[4]Vollmers, H., and Rotta, J. C., "Similar Solutions of the Mean Velocity, Turbulent Energy and Length Scale Equation," *AIAA Journal*, Vol. 15, No. 5, 1977, pp. 714–720.

[5]Paullay, A. J., Melnik, R. E., Rubel, A., and Siclari, M. J., "Similarity Solution for Plane and Radial Jets Using a $k$-$\epsilon$ Turbulence Model," *Journal of Fluids Engineering*, Vol. 107, March 1985, pp. 79–85.

[6]Abid, R., and Speciale, C. G., "Application of a New $K$-$\tau$ Model to Near Wall Turbulent Flows," AIAA Paper 91-0614, Jan. 1991.

# Stability of Plane Nonorthogonal Stagnation Flow

J. M. Floryan*
*University of Western Ontario,*
*London, Ontario, N6A 5B9 Canada*

## I. Introduction

THE problem of stability of stagnation flow is of continuous interest in aerospace applications mainly because this flow well approximates flows around leading edges of airfoils. It is widely believed that this flow is linearly stable.[1] Recent numerical simulations of Spalart[2] show this flow to be also nonlinearly stable. Experiments[3] demonstrate close coupling between the form of the oncoming disturbances and the secondary flow observed in the stagnation region; however, the mechanism of this coupling is not completely understood. Certain aspects of this coupling can be explained on the basis of the "vorticity amplification theory."[4] Possible roles of surface roughness have been discussed in Ref. 5. It is likely that the flow realized in experiments is nonorthogonal, or perhaps disturbances swept toward the body produce instantaneous nonorthogonality, which is sufficient to trigger the secondary flow. The objective of the present analysis is, therefore, to determine stability characteristics of such a nonorthogonal flow.

Received July 10, 1991; accepted for publication Aug. 14, 1991.

*Professor, Department of Mechanical Engineering.

## II. Analysis

We consider motion of a viscous fluid impinging obliquely on an infinite flat rigid wall. The geometry of the flow and the coordinate system are indicated in Fig. 1. The wall is in the $(x, z)$ plane, and the mean flow is two dimensional in the $(x, y)$ plane. The oncoming flow has the form

$$u^* = ax^* + 2aHy^*, \qquad v^* = -ay^* \tag{1}$$

i.e., it consists of a superposition of an irrotational stagnation-point flow and a uniform shear parallel to the wall with constant $z$ component of vorticity ($\omega_z = 2H$). In the previous equation, $u$ and $v$ denote velocity components in the $(x, y)$ directions, asterisks denote dimensional quantities, and $a$ and $H$ are scale constants. The angle of inclination of the flow with respect to the wall is $\beta = \arctan H^{-1}$.

We are interested in the character of the flow in the viscous layer next to the rigid wall when the far-field approximation is given by Eq. (1). This problem has been studied in Refs. 6–8. The following presentation is limited to a short outline.

Boundary-layer thickness $\delta$, upstream velocity $V_\infty$, and dynamic pressure $\rho V_\infty^2$ associated with the orthogonal stagnation-point flow are selected as the length, velocity, and pressure scales, respectively. Here, $\delta = (\nu/a)^{1/2}$ where $\nu$ denotes kinematic viscosity and $\rho$ stands for density. The Reynolds number is defined as $Re = V_\infty \delta/\nu$. Flow quantities are expressed as

$$U(x,y) = 1/Re\left[xU_0(y) + HU_1(y)\right], \quad V(x,y) = 1/Re V_0(y)$$
$$P_0 - P(x,y) = 1/Re^2\left[\tfrac{1}{2}x^2 + G_0(y)\right] \tag{2}$$

where $U$ and $V$ are the mean flow velocity components in the $(x, y)$ directions, $P$ denotes the mean flow pressure, and $P_0 = P(0,0)$. If we define

$$U_0 = \frac{\mathrm{d}F}{\mathrm{d}y}, \qquad V_0 = -F \tag{3}$$

and substitute Eqs. (2) and (3) into the incompressible Navier-Stokes and continuity equations, we find that $F$, $G_0$, and $U_1$ must satisfy

$$\frac{\mathrm{d}^3F}{\mathrm{d}y^3} + F\frac{\mathrm{d}^2F}{\mathrm{d}y^2} - \left(\frac{\mathrm{d}F}{\mathrm{d}y}\right)^2 + 1 = 0 \tag{4a}$$

$$G_0 = \frac{\mathrm{d}F}{\mathrm{d}y} + \frac{1}{2}F^2 \tag{4b}$$

$$\frac{\mathrm{d}^2U_1}{\mathrm{d}y^2} + F\frac{\mathrm{d}U_1}{\mathrm{d}y} - \frac{\mathrm{d}F}{\mathrm{d}y}U_1 = 0 \tag{4c}$$

$$F = \frac{\mathrm{d}F}{\mathrm{d}y} = U_1 = 0 \quad \text{at } y = 0 \tag{4d}$$

$$\frac{\mathrm{d}F}{\mathrm{d}y} \to 1, \qquad U_1 \to 2Y \quad \text{as } y \to \infty \tag{4e}$$